

Characterisation of liquid transfer processes and water adsorption mechanism on a porous ceramic by acoustic emission means

T. Chotard^{a,b,*}, A. Smith^{a,*}, A. Quet^a

^a *Groupe d'Etude des Matériaux Hétérogènes (GEMH, EA 3178), Ecole Nationale Supérieure de Céramique Industrielle, 47 à 73 Avenue Albert Thomas, 87065 Limoges Cedex, France*

^b *Institut Universitaire de Technologie, Département Génie Mécanique et Productique, 2 allée André Maurois, 87065 Limoges Cedex, France*

Available online 16 June 2006

Abstract

In this paper, some applications of acoustic emission (AE) technique to characterise the liquid transfer mechanisms during drying process of a porous ceramic are presented and discussed. Results are compared with the general theory of drying and a more recent approach dealing with thermodynamic modelling itself based on capillary stresses and hygromechanical coupling. The sensitivity of the acoustic emission technique to the energy release processes acting during liquid transfer in a porous material (sorption and desorption) has been emphasised and the hysteretic phenomenon in a porous ceramic has been illustrated. Based on the experiments, the relationship between the AE characteristics recorded during the tests and the different mechanisms, which take place during drying process, was underlined. Information deduced from AE measurements associated with other data obtained from weight-loss measurements enable to propose a qualitative description of drying chronology.

© 2006 Elsevier Ltd. All rights reserved.

Keyword: Silicate; Drying; Interfaces; Acoustic emission

1. Introduction

Understanding how liquid flows through a porous body^{1–5} is an issue that has been studied academically in many different fields: soil mechanics,⁶ saturated porous media for oil prospecting⁷ or storage of polluting agents.⁸ Recent work concerns the characterisation of transfer moisture in building materials.⁹ The experimental approaches that have been developed are mostly based on ultrasonic techniques.¹⁰ In the present case, we have applied acoustic emission (AE). Indeed, this technique is sensitive to energy release phenomenon that induces elastic waves propagation in a material submitted, for example, to stresses. In the case of cements or plasters hydration and setting, where drying is involved, data have shown that it is active in acoustic emission.¹¹ This paper is devoted to the study by AE of water adsorption in a porous ceramic material and its drying after impregnation with water.

2. General theory of drying

2.1. Phenomenological description

The principle of flow in porous bodies is relatively simple but its analysis is rather complicated.¹² Liquid flows through a porous medium in response to a gradient in pressure. At the same time, the pressure induces deformation of the solid skeleton and dilatation of the pores through which the liquid moves. To better understand the global chronology of drying phenomenon and stages involved in process are detailed below.

2.1.1. Chronology of stages

Considering a porous medium saturated with a liquid, the drying process can be divided into three periods, as illustrated in Fig. 1.

The first stage, called the constant rate period, is when evaporation occurs only from the surface of the pore. During this stage, the rate of evaporation per unit area of the drying surface is independent of time and is the same as for a free water surface. The liquid/vapour interface, or meniscus, remains at the exterior surface of the body but its radius decreases con-

* Corresponding authors.

E-mail addresses: t.chotard@ensci.fr (T. Chotard), a.smith@ensci.fr (A. Smith).

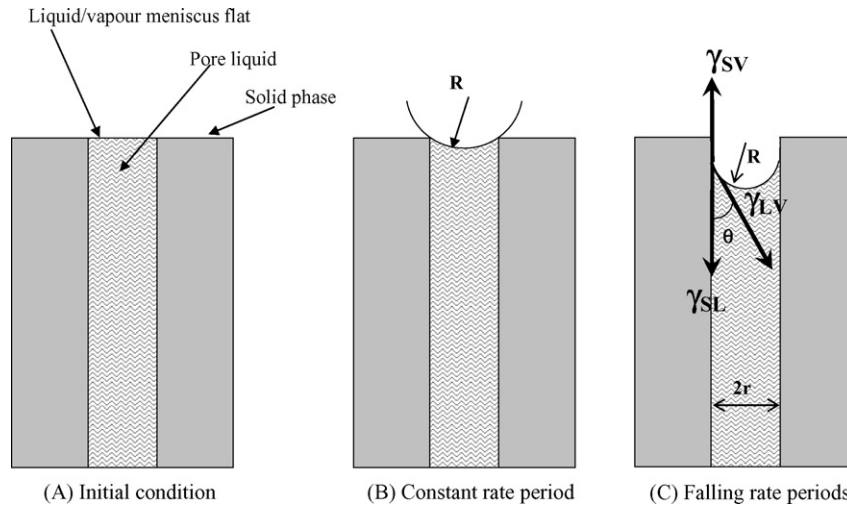


Fig. 1. Schematic illustration of the general chronology of drying process for a pore: (A) initial condition; (B) constant rate period; (C) falling rate periods.

tinuously, due to evaporation. The liquid is in tension and the solid phase is in compression, which may cause shrinkage in deformable systems. At the end of this period, called the critical point, the radius of the meniscus becomes equal to the radius of the pore and the compressive forces exerted on the solid are at the maximum.

The second step is called the first falling rate period. Just beyond the critical point, the radius of curvature of the meniscus is small enough to enter the pores and the liquid recedes into the pores. During this period, the rate of evaporation decreases and is sensitive to the ambient temperature and vapour pressure. Compressive forces, and consequently shrinkage, in deformable solids, virtually stop. The liquid in the pores located near the surface flows to the outside and evaporates from the external surface. At the same time, part of the liquid can evaporate within the pores and the vapour is diffused to the surface. This situation is characterised by coupled effects, namely liquid flow and diffusion of vapour.

The third stage is called the second falling rate period. As drying progresses, some of the liquid water cannot reach the surface (due to the deep penetration of the liquid meniscus in the porous network) and has to evaporate within the pores. As the saturated area retracts into the body, the solid skeleton is submitted to differential strains induced by a gradient of stress in the medium (compression in the saturated region is higher than near the drying surface).

2.1.2. Forces on the solid and transport mechanisms of the liquid

The capillary pressure. During the first stage of drying, the capillary pressure, P_c (i.e. the tension in the liquid), is directly related to radius of curvature (R) of the meniscus through Laplace's law:

$$P_c = \frac{-2\gamma_{LV}}{R} \quad (1)$$

where γ_{LV} is the liquid/vapour interfacial energy (or surface tension). The sign of the capillary pressure is related to the sign

of the radius of curvature. When the centre of curvature is located in the vapour phase, R is negative, P_c is positive and the liquid is in tension. The maximum capillary pressure (P_R) occurs when R is sufficiently small to enter the pore. The minimum value of R for a cylindrical pore with a radius r is given by

$$R = -\frac{r}{\cos \theta} \quad (2)$$

where θ is the contact angle exhibiting the wet ability of the liquid. For real pores (non-cylindrical), P_R is related to the surface-to-volume ratio of the pore space S_P/V_P :

$$P_R = \frac{(\gamma_{SV} - \gamma_{SL})S_P}{V_P} = \frac{\gamma_{LV} \cos \theta S_P}{V_P} \quad (3)$$

where γ_{SV} and γ_{SL} are the solid/vapour and solid/liquid interfacial energies. When examining the surface-to-volume ratio of the pore, we can see that it is related to the specific surface area of a porous body by

$$\frac{S_P}{V_P} = \frac{S \rho_s \rho}{1 - \rho} \quad (4)$$

where ρ is the relative density, $\rho = \rho_b/\rho_s$, ρ_b is the bulk density of the solid network (not considering the mass of liquid) and ρ_s is the density of the solid skeleton.

Fluid flow through porous media follows Darcy's law which affirms that the flux of liquid, J , is proportional to the gradient in pressure in the liquid, ∇P_L :

$$J = -\frac{D}{\eta_L} \nabla P_L \quad (6)$$

where D is the permeability (in units of area) and η_L is the viscosity of the liquid. The factor of 5 is empirical and corrects the non-circular section of real pores.

During evaporation, a part of the vapour is transported by diffusion that obeys to Fick's law where the diffusive flux (J_D) is proportional to the concentration gradient (∇C):

$$J_D = -D_C \nabla C \quad (8)$$

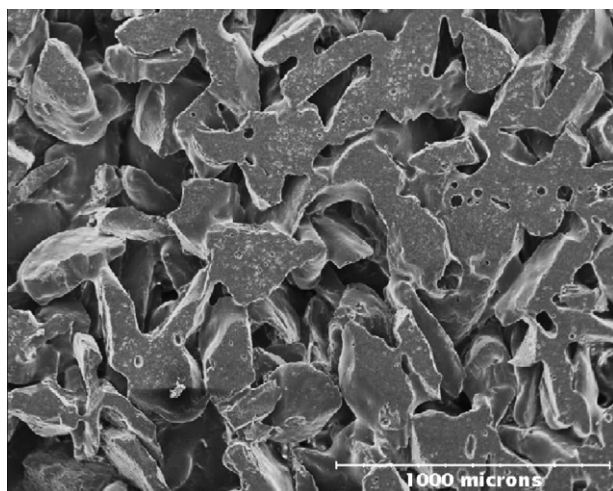


Fig. 2. Scanning electron micrograph of the porous ceramic.

where D_C is the chemical diffusion coefficient and C the concentration. In this study, we will only focus on flow process.

3. Experimental procedure

3.1. Material

The porous material used in our work is a cylindrical silica–alumina sintered ceramic sample, with a diameter and a height of 100 and 10 mm, respectively. The porous characteristics have been measured by mercury porosimetry measurement. The cumulative open porous volume is of the order of 33 vol.%. The pore size ranges mainly between 70–80 and 200–300 μm and a small percentage of pores between 5 and 20 nm. A micrograph by scanning electron microscopy reveals that the large pores correspond to intergranular porosity while the small ones are within the grains (Fig. 2). Lastly, the micrometric porous network is rather tortuous. In order to study adsorption and drying phenomena, this porous material has been selected because it

has a large porous volume and consequently, the surface developed by the interior of the pores is about 10^3 times greater than the outer surface of the ceramic.

3.2. Experimental setup

The acoustic emission system used in this study is a AEDSP-32/16 MISTRAS digital system from Physical Acoustics Corporation. This system allows the waveform and the main feature parameters well known in AE study such as count, hit, rise time, duration of hit, count to peak, amplitude (in dB), to be recorded. The plug-in filter of this system has a bandwidth from 100 to 1200 kHz. Two sensors (PAC MICROPHONE R15), one test sensor and one reference sensor, with a bandwidth from 50 to 250 kHz, are connected through preamplifiers (EPA 1220A). The reference sensor is used in order to record noises due to the electromagnetic environment and to eventually subtract these parasite signals from the one recorded on the test sensor. The preamplifiers provide 40/60 dB gain (switch select) and operate with either single ended or differential sensor. A coupling fluid (Dough 428 Rhodorsil Silicone) is used to have an airless and flawless contact between the transducer and the specimen. For all the experiments, the specimens are placed in a special chamber, where the temperature and the relative humidity (RH) are controlled (Fig. 3). Experiments were conducted either at atmospheric pressure (1 atm) or at a pressure of 10^{-2} atm.

Prior to experiments, the porous ceramic has been heated at 110 °C for 1 h and then stored under dry nitrogen at room temperature. This protocol has been applied in order to minimize the amount of water already adsorbed in the ceramic surface before testing. Two series of experiments have been carried out. In the first series, the ceramic is placed in different relative humidities of water and different pressures and is referred as “non-impregnated porous material”. In the second series, the porous ceramic is impregnated with water under vacuum for a minimum of 4 h by several kinds of liquids; it is referred as “impregnated porous material”.

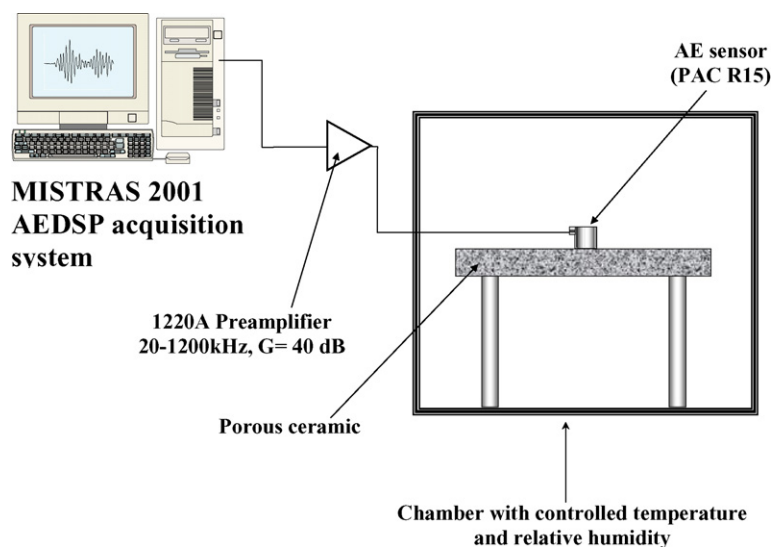


Fig. 3. Experimental setup for drying testing of a porous ceramic.

Table 1
AE features for non-impregnated porous media tested with different RH levels

Pressure = 1 atm	Hit rate ($\partial(\text{hit})/\partial t$) (h^{-1})	Cumulated number of hits after 20 h
RH = 10%	1.4	25
RH = 40%	6.9	119
RH = 90%	32.9	657

4. Results and discussion

4.1. Results for non-impregnated porous material

Prior to AE experiments on the porous ceramic, a first test was carried out at 90% relative humidity and 1 atm on a specimen of similar dimensions made with stearic acid which is well known for its hydrophobic properties (no water adsorption). Only one hit was recorded during a period of 20 h. This result shows that in our experimental conditions, there is no parasitic signal.

4.1.1. Influence of the relative humidity and pressure level

The first testing campaign was performed on the ceramic free of fluid and placed inside the chamber at atmospheric pressure (1 atm) with three relative humidities, namely 10, 40 and 90%. Each test has been performed three times and was found to be quite reproducible.

From these data, some interesting comments can be done. Firstly, we can note that for all humidity levels, the acoustic activity starts from the very beginning of the test, even for the lowest RH level. According to Table 1, it seems that both the total amount of hits during the test and the hit rate ($\frac{\partial(\text{hit})}{\partial t}$) are closely related to the level of relative humidity. In fact the test under the highest RH level (90%) exhibits a maximum value around 650 hits after 20 h while the experiment under the lowest RH level (10%) reaches a maximum amount of 20 hits after the same duration. At this stage of the study, it is important to remember that the porous material has been installed inside the testing chamber without being impregnated by any fluid and that, prior to AE measurements, it has been treated for 1 h at 110 °C and kept at room temperature in neutral atmosphere (dry nitrogen). Taking into account all these parameters, it seems that the acoustic emission is induced by an interaction between water molecules and the surface of the porous medium. Indeed, the more the RH level increases, the more the atmosphere inside the cell contains water molecules and the more the surface of the porous medium is able to fix these molecules on its surfaces.

The water adsorption at the external surface of a pore is a process that changes the nature of the interface. In fact, the solid/vapour interface is replaced by a less energetic solid/liquid interface. This change leads to a release of energy (even at a very small level), which is transformed partly, into mechanical waves propagating through the microstructure, and in other into thermal flow.

Another testing campaign has been conducted on the same kind of porous ceramic with the same preparation protocol. The RH level is, this time, fixed at 90% and the pressure level in the chamber decreased from atmospheric pressure to 10^{-2} atm.

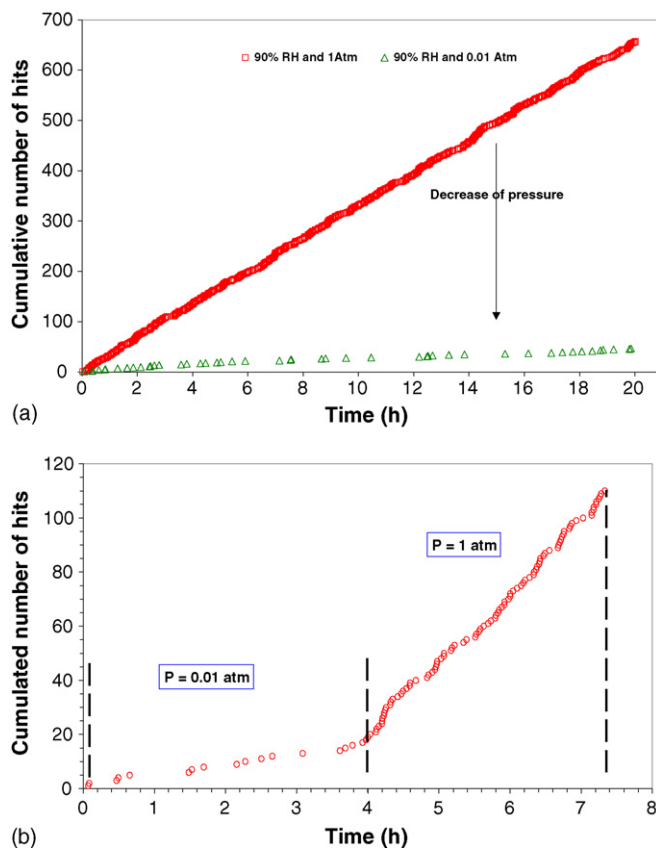


Fig. 4. (a) Evolution of the acoustic activity of a non-impregnated porous medium: (a) for different pressures (RH=90%); (b) with two pressure levels: 0.01 atm from 4 h, 1 atm beyond 4 h (RH=90%).

We assume that the pressure variation has no incidence on the deformation of the solid skeleton.

Fig. 4 shows both the differences in maximum cumulated level and in hit rate (657 hits and 33 hits/h under atmospheric pressure, 47 hits and 2 hits/h for the test under 10^{-2} atm, respectively). The highest level in pressure exhibits the highest values of these AE features. Another experiment was conducted under 90% RH (Fig. 4b). The pressure was initially equal to 0.01 atm and raised to 1 atm after 4 h. The value of the hit rate is clearly different before and after the pressure; it is equal to 4 and 27 hits/h, respectively. These values are of the same order of magnitude than those deduced from the experiments at a given pressure (2 hits/h under 10^{-2} atm and 33 hits/h under 1 atm, Fig. 4a). According to the gas kinetics theory,¹³ the flow F of molecules (in molecules $\text{cm}^{-2} \text{s}^{-1}$) hitting a unit area (cm^2) depends on the temperature T (°C), the pressure P (Pa), the average molar weight M (g mol^{-1}) of the considered molecules and the Avogadro number (N_a):

$$F = \frac{N_a P}{\sqrt{2\pi M R_g T}} \quad (9)$$

where R_g is the perfect gas constant.

According to this equation, an increase in pressure P will lead to an increase in the flow F of molecules. If we still consider the hypothesis that the adsorption of water molecules is closely related to the acoustic activity recorded during the test,

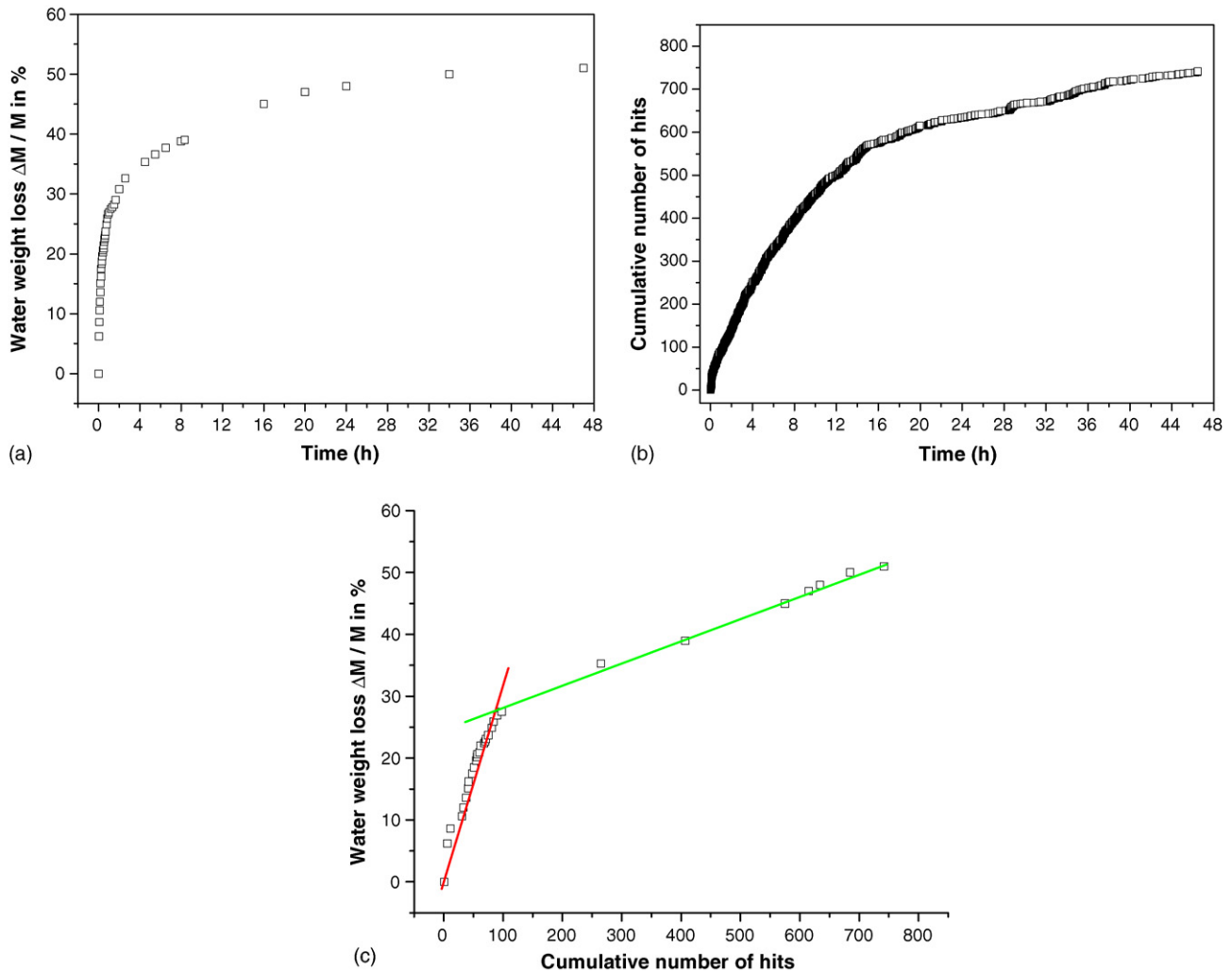


Fig. 5. (a) Evolution of the relative weight loss of a water impregnated porous medium during drying ($RH=90\%$, $P=1$ atm, $T=23^\circ\text{C}$). (b) Evolution of the acoustic activity of a water impregnated porous medium during drying ($RH=90\%$, $P=1$ atm, $T=23^\circ\text{C}$). (c) Variation of the relative water weight loss as a function of the cumulated number of hits during drying test of impregnated porous ceramic ($RH=90\%$, $P=1$ atm, $T=23^\circ\text{C}$).

the lower the pressure is, the lower is the recorded AE activity. In conclusion, the AE technique can be a useful tool to monitor adsorption of water on solid surfaces.

4.2. Results for impregnated porous medium

4.2.1. Drying tests results

The porous ceramic is initially impregnated with water and placed on a piece of blotting paper in order to ensure a good emptying of the pores during the test. The experiments have been conducted at room temperature (23°C), RH of 90% and under 1 atm. Prior to AE testing, the water weight loss of the porous medium has been measured under the same configuration. Fig. 5a presents the variation of the relative water weight loss as a function of time. As we can see here, the weight loss rate is rather high during the first hour ($25.3\%/h$). After 1 h, the slope of the curve is slightly reduced and after 48 h, the relative water weight loss reaches its maximum value, near 50%. The test is conducted at a high RH level (90%), which can explain the high value of the relative water amount that still remains in the

porous ceramic after 48 h. Fig. 5b shows the evolution of the cumulated number of hits for the same sample under the same testing configuration. According to this figure, the variation of the acoustic activity seems to be closely related with the evolution of the relative water weight loss (Fig. 5a). To illustrate this correlation, Fig. 5c presents, on a first approximation, the variation of the relative water weight loss as a function of the cumulated number of hits. As we can see in this figure, the curve exhibits some proportional behaviour. This could be interpreted as follows.

The proportional variations can be related to single mechanism acting during drying. If we assume that this mechanism is the flow of liquid produced by the movement of the meniscus in the pore (first falling rate period), the kinetic energy produced by this motion can generate the propagation of mechanic waves that can give an acoustic activity. The change in the slope (the slope is greater before 100 cumulated hits than after) can be interpreted as a change in the dimension of the pores that are being emptied. As said before, the pore size ranges between 70–80 and 200–300 μm . The porous ceramic is also

placed on a blotting paper during test; which can act as a pumping device that accelerates the emptying of the pores. If we consider that the AE activity is due to the emptying of pores, the draining of water in the largest (resp. smallest) pores will give acoustic emission activity first (resp. second) as time goes on.

If we consider now that the dimensions of the pores are not too different, another interpretation can be done. As we have seen before, the first falling rate period is when the meniscus retreats into the pore and the liquid is in its funicular state (continuous liquid). During this stage, transport by liquid flow is possible and some diffusion occurs too. The remaining question is whether these two mechanisms can release energy and induced acoustic activity in the ceramic.

In terms of energy, and according to Coussy's work,^{13,14} about the detailed description of the thermodynamics of liquid transfer processes in porous media, one can say that there are some close correlations between the hypothesis above proposed presenting the onset of an acoustic emission activity and the different phenomena that occur during the drying process of a porous medium.

5. Conclusion

Liquid transfer processes have been investigated by acoustic emission. This paper describes the monitoring of drying of a porous ceramic and the AE characterisation of several mechanisms involved in this phenomenon. Qualitative observations and quantitative measurements allow to propose some concluding remarks:

- AE technique is able to detect low energy processes acting at the molecule scale (surface adsorption of water on pore).
- A quantitative correlation has been found between the AE activity and the water weight loss of the porous medium during drying. These two last observations clearly show that this technique is able to characterise drying phenomena in a large-scale range (from nanoscopic to microscopic scale). Distinct AE signatures have been identified for the different processes.
- The hypothesis presented in the general theory of drying and its thermodynamical approach are in good accordance with the AE measurements. This result tends to demonstrate that the acoustic activity recorded during drying tests is directly

related to the energy release of the system induced by the change in surface energy and the motion of the fluid (flow and movement of the meniscus).

Lastly, the important advantage of this non-destructive, in situ and real time technique is that it can be applied to follow the drying process of fairly large real specimens (cement, mortars or concrete). Future works will deal with the frequency analysis of the acoustic emission signals in order to investigate the wave propagation through this multiphase medium.

References

1. Van Breugel, K., Simulation of hydration and formation of structure in hardening cement based materials, PhD Thesis, Delft University of Technology, 1991.
2. Bentz, D. P. and Hansen, K. K., Preliminary observation of water movement in cement pastes during curing X-ray absorption. *Cem. Conc. Res.*, 2000, **30**, 1157–1168.
3. Hansen, K. K. and Bentz, D. P., Studies of hydration and drying in cement pastes by scanning X ray absorptiometry. In *Proceedings of the water in cement paste and concrete—hydration and pore structure workshop*, 1999, pp. 107–114.
4. Scherer, G., Effect of drying on properties of silica gel. *J. Non. Cryst. Sol.*, 1997, **215**, 155–168.
5. Nielsen, E., Einarsrud, M. A. and Scherer, G., Effect of precursor and hydrolysis conditions on drying shrinkage. *J. Non. Cryst. Sol.*, 1997, **221**, 135–143.
6. Weinberger, R., Initiation and growth of cracks during desiccation of stratified muddy sediments. *J. Struct. Geo.*, 1999, **4**(21), 379–386.
7. Boutin, C. and Auriault, J. M., Dynamic behaviour of porous media saturated by a viscoelastic fluid. Application to bituminous concretes. *Int. J. Eng. Sci.*, 1990, **28**(11), 1157–1181.
8. Mironova, M., Gospodinov, P. and Kazandjiev, R., The effect of liquid push out of the material capillaries under sulphate ion diffusion in cement composites. *Cem. Conc. Res.*, 2002, **32**, 9–15.
9. Baroghel-Bouny, V., Mainguy, M., Lassabatere, T. and Coussy, O., Characterisation and identification of equilibrium and transfer moisture for ordinary and high-performance cementitious materials. *Cem. Conc. Res.*, 1999, **29**, 1225–1238.
10. Auriault, J. M. and Lebaigue, O., Acoustic waves in a mixture of fluids with capillary effects. *Int. J. Eng. Sci.*, 1989, **27**(10), 1253–1265.
11. Chotard, T., Smith, A., Rotureau, D., Fargeot, D. and Gault, C., Acoustic emission characterisation of calcium aluminate cement hydration at the early age. *J. Eur. Ceram. Soc.*, 2003, **23**, 387–398.
12. Scherer, G., Theory of drying. *J. Am. Ceram. Soc.*, 1990, **73**, 3–14.
13. Coussy, O., Thermodynamics of saturated porous solids in finite deformations. *Eur. J. Mech. A: Solids*, 1989, 1–14.
14. Coussy, O., *Mechanics of porous continua*. John Wiley and Sons, 1995.